

X-Cube Model on Generic Lattices: New Phases and Geometric Order

Kevin Slagle¹ and Yong Baek Kim^{1,2}

¹*Department of Physics, University of Toronto,
Toronto, Ontario M5S 1A7, Canada*

²*Canadian Institute for Advanced Research,
Toronto, Ontario, M5G 1Z8, Canada*

Fracton order is a new kind of quantum order characterized by topological excitations which exhibit remarkable mobility restrictions and a robust ground state degeneracy (GSD) which can increase exponentially with system size. In this manuscript, we present a generic lattice construction (in three dimensions) for a generalized X-cube model of fracton order, where the mobility restrictions of the subdimensional particles inherit the geometry of the lattice. This helps explain a previous result that lattice curvature can produce a robust GSD, even on a manifold with trivial topology. We provide explicit examples to show that the (zero temperature) phase of matter is sensitive to the lattice geometry. In one example, the lattice geometry confines the dimension-1 particles to small loops, which allows the fractons to be fully mobile charges, and the resulting phase is equivalent to 3+1D toric code. However, the phase is sensitive to more than just lattice curvature; different lattices without curvature (e.g. cubic, stacked kagome, or even just a rotated cubic lattice) also result in different phases of matter, which are separated by phase transitions. (Models on different lattices can be compared by adding trivial gapped qubits so that both models share the same Hilbert space.) Thus, the long distance physics of the X-cube model (i.e. its phase, subdimensional particles, and GSD) is highly sensitive to lattice geometry. This greatly contrasts (liquid) topologically ordered models, such as toric code, which are blind to lattice geometry (and only sensitive to topology). We therefore propose that fracton orders should be regarded as a *geometric order*.

Topologically ordered quantum phases of matter are often characterized by their topological excitations [[1]] and topological ground state degeneracy (GSD). These (liquid [2]) topological phases [3–5] (e.g. Z_2 gauge theory described by toric code [6] or BF theory [7, 8]) are topologically invariant. That is, the Lagrangian has no dependence on the spacetime metric; the GSD only depends on the topology of the spatial manifold; and the braiding statistics of the topological excitations only depends on the topology of the braiding paths.

This topological invariance is absent in the recently discovered, exactly solvable, gapped 3D lattice models [9–20] that exhibit so-called fracton topological order [14]. Fracton order can be characterized by its topological excitations which are subdimensional [21], which means that they are immobile or are restricted to only move along lines or surfaces without creating or destroying other topological excitations. The immobile excitations are called fractons, while the particles that are bound to lines and surfaces are called dimension-1 particles (or lineons [22]) and dimension-2 particles, respectively. Fracton order has also been characterized by its GSD which increases exponentially with system size on a torus [9, 10, 23], geometric braiding processes (Fig. 1), geometry-dependent entanglement [24–26], glassy dynamics [12, 27, 28], duality to lattice defects [29], duality to fractal and subdimensional symmetry breaking [11, 14, 30, 31], bifurcation in entanglement renormalization [23, 32], and connections to emergent gravity [33].

The aim of our work is to demonstrate the significance of geometry in the study of fracton order by considering the effects of changing the geometry of the lattice. By

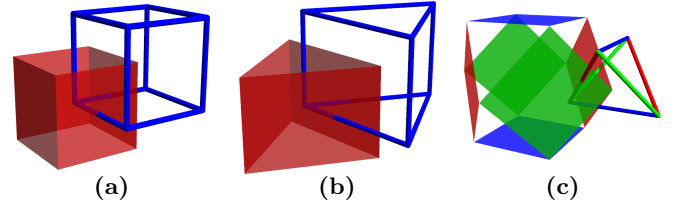


FIG. 1. Geometric braiding operators for the (a) X-cube model on a cubic lattice [14, 16, 34], (b) X-cube model on a stacked kagome lattice, and (c) Chamon model [12, 13] of fracton order. The surfaces are membrane operators that braid fractons around the edge of the membrane by exchanging other excitations in the interior of the membrane [34]. The lines are string operators that braid dimension-1 particles. The operators are products of X , Y , and Z Pauli operators, which are colored red, green, and blue. Thus, in fracton orders, the braiding paths of the subdimensional excitations must take rigid geometric shapes that depend on the model and lattice.

lattice geometry, we mean: Is the lattice a cubic lattice or stack of kagome lattices? Or does the lattice have curvature (as in e.g. Fig. 5)? Although liquid topological order (e.g. Z_2 gauge theory) is completely blind to lattice geometry, we will show that lattice geometry plays a fundamental role in the physics of fracton order. To do this, in Sec. II we formulate a lattice construction (Fig. 3) of generic lattices on which we can define a generalized X-cube fracton model, which was previously only defined on a cubic lattice [14].

In Sec. III we will see that the mobility restrictions of the subdimensional particles inherit the geometry of the lattice. This helps explain a previous discovery

that lattice curvature can result in a robust GSD on a manifold with trivial topology (Fig. 6b) [34].

In Sec. IV, we show that the lattice geometry can also affect the phase of matter (at zero temperature). As examples, we consider two lattices (Fig. 8 and 7) where the geometry grants fractons either full or subdimensional mobility which results in a phase equivalent to 3+1D Z_2 gauge theory or a stack of 2+1D toric codes.

In Sec. V, we show that the phase is sensitive to more than just lattice curvature. For example, the X-cube model on different lattices without curvature (e.g. cubic or stacked kagome) can result in a different GSD. Remarkably, we show that a rotated lattice can also correspond to a different phase; i.e. the X-cube model on cubic lattices with different orientations corresponds to different phases of matter. The phases are different in the sense of Ref. [35] (and [36]). That is, the ground state wavefunctions differ by more than just a finite local unitary transformation; equivalently, any adiabatic evolution from one Hamiltonian to the other must cross a phase transition (Fig. 9). (Hamiltonians on different lattices can be compared by adding trivial gapped qubits so that both Hamiltonians share the same Hilbert space.) This surprising result can be understood from the fact that different lattices have different lines and surfaces that the subdimensional particles are bound to (Fig. 11). Therefore, the lattice geometry used to define the X-cube model significantly affects the phase of matter.

I. X-CUBE MODEL REVIEW

The X-cube model was originally defined on a cubic lattice with Z_2 Pauli operators on the links [14]:

$$H_{\text{X-cube}} = - \sum_{\text{cube}} \prod_{\ell \in \text{cube}} Z_{\ell} - \sum_{+} \prod_{\ell \in +} X_{\ell} \quad (1)$$

The first term sums over all cubes in the lattice and is a product of 12 Pauli Z operators over the 12 edges of the cube (Fig. 2a). Excitations of this term are immobile fractons which are created at the corners of rectangular membrane operators [14]. However, a pair of neighboring fractons is a dimension-2 particle which can move along a plane (via the same “membrane” operator but of unit width). This cube operator counts the number of fractons within the cube by braiding dimension-1 particles (excitations of the second term) around the edges of the cube.

The second term in the Hamiltonian sums over all quadruples of links which make the shape of a cross and is a product of 4 Pauli X operators over these 4 links (Fig. 2b). Excitations of this term are dimension-1 particles which can only move along the x, y, or z axes [14]. The collection of an x-axis, y-axis, and z-axis dimension-1 particle can fuse into the vacuum. A

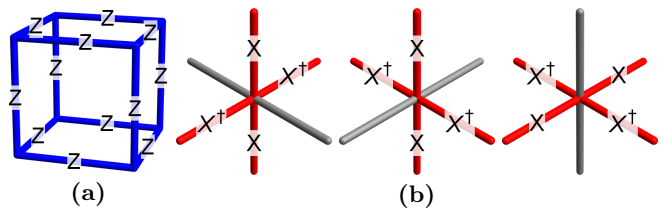


FIG. 2. (a) For every cube, the X-cube model on a cubic lattice (Eq. (1)) has a 3-cell operator which is a product of 12 Pauli Z operators along the edges of the cube: $\prod_{\ell \in \text{cube}} Z_{\ell}$. (b) At each vertex, there are three cross operators: one for each of the three planes that intersect the vertex. The operators are a product of four X operators on the four links within the plane that neighbor the vertex: $\prod_{\ell \in +} X_{\ell}$. (Regarding daggers in figure: [[37]].)

neighboring pair of dimension-1 particles moving in the same direction is a dimension-2 particle, which can move along the plane orthogonal to their displacement. The cross operator in the XY plane counts the number of x-axis and y-axis particles at the vertex (modulo 2) by braiding an XY-plane fracton pair around a loop in the XY plane.

II. INTERSECTING SURFACES LATTICE CONSTRUCTION

Unlike liquid topological order, the X-cube model can not be naturally defined on an arbitrary lattice. The links neighboring each vertex must come in pairs to uniquely specify how a dimension-1 particle should pass through a link. We may also want to preserve the fusion rule that the collection of three orthogonal dimension-1 particles can fuse into the vacuum. Thus, we will restrict the vertices to have exactly six neighboring links so that there are exactly three kinds of dimension-1 particles at each vertex. Therefore, each vertex must locally look like the vertex of a cubic lattice. Additionally, there must be a notion of surfaces for the dimension-2 particles to be bound to.

In order to facilitate these conditions, we will construct our lattice from a collection of intersecting surfaces, which we will refer to as i-surfaces. The motion of a dimension-2 fracton pair will be restricted to these i-surfaces. The dimension-1 particles will traverse the lines formed by the intersection between two i-surfaces. The lattice has a vertex wherever three i-surfaces intersect. Links between vertices are places where two i-surfaces intersect. As desired, not all lattices are compatible with this construction; e.g. a stack of honeycomb lattices can't be constructed, which is sensible since it is not clear how a dimension-1 particle should pass through a 5-valence vertex of a stacked honeycomb lattice. For simplicity, we will require that the i-surfaces are not fine tuned; i.e. perturbing the i-surfaces should not change the

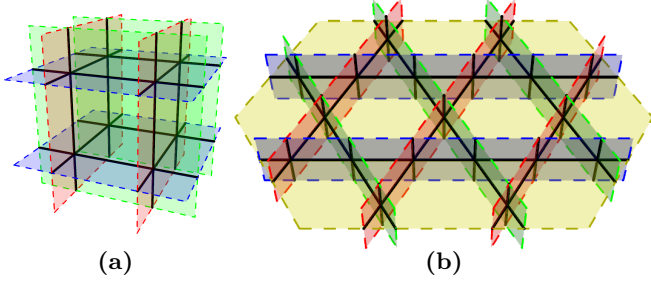


FIG. 3. (a) A cubic lattice and (b) a stack of kagome lattices constructed from intersecting surfaces (colored planes), which we refer to as i-surfaces. Pauli operators live on the links (black) of the lattice, which are placed where two i-surfaces intersect. The Hamiltonian (Eq. (2)) consists of three cross operators at each vertex (Fig. 2b), and a 3-cell operator at each 3-cell (3D volume enclosed by i-surfaces) which is a product of Z operators on the edges of the 3-cell. The stack of kagome lattices has two kinds of 3-cells: a triangular prism (Fig. 4a) and a hexagonal prism.

lattice. This implies that no more than three i-surfaces can intersect at a single point and no more than two i-surfaces can intersect along a line (which e.g. rules out a stack of triangular lattices). As examples, in Fig. 3 we show how this construction can form a cubic lattice or stack of kagome lattices.

The Hamiltonian is:

$$H_{\text{X-cube}} = - \sum_{\text{cube}} \prod_{\ell \in \text{cube}} Z_{\ell} - \sum_{+} \prod_{\ell \in +} X_{\ell} \quad (2)$$

$$- \sum_{\bigcirc} \prod_{\ell \in \bigcirc} Z_{\ell} - \sum_{\odot} \prod_{\ell \in \odot} X_{\ell}$$

The first two terms generalize Eq. (1). Instead of summing over cube operators in the first term, we instead sum over all 3-cells (3D volumes enclosed by i-surfaces) at which the 3-cell operator is a product of Z operators on the edges of the 3-cell (Fig. 4a). The second term again consists of three cross operators at each vertex, one for each of the three i-surfaces intersecting the vertex (Fig. 2b). The third term sums over all finite-sized loops (that don't increase in size as the system size increases) and is a product of Z operators around the loop (Fig. 4b). The fourth term sums over all finite-sized parallel loops and is a product of X operators on the links connecting the parallel loops (Fig. 4c). The last two terms are new, and only appear when there are finite-sized intersections between i-surfaces. Without the last two terms, the model can be fine tuned (e.g. in Fig. 7). [[38]]

III. SIGNIFICANCE OF GEOMETRY

Now that we can define the X-cube model on different lattices, we can ask: How does the geometry of the lattice affect the long distance physics?

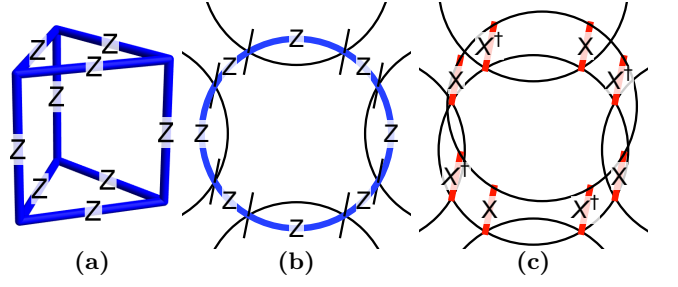


FIG. 4. New kinds of X-cube Hamiltonian terms in Eq. (2). (a) An example of a 3-cell operator on a triangular prism, which is a 3-cell in a stack of kagome lattices (Fig. 3b). The 3-cell operator ($\prod_{\ell \in \text{cube}} Z_{\ell}$) on a 3-cell (cube) is a product of Z operators on the links around the edges of the 3-cell. (b) A product of Z operators on the links around a loop: $\prod_{\ell \in \bigcirc} Z_{\ell}$. (c) A product of X operators on links connecting two parallel loops: $\prod_{\ell \in \odot} X_{\ell}$. (Regarding daggers in figure: [[37]].)

For the case of liquid topological orders, such as Z_2 gauge theory which is described by toric code or BF theory, the geometry of the lattice or curvature of the spatial manifold has little effect on the long distance physics. That is, it doesn't matter if toric code is defined on a square lattice or triangular lattice; the charge and flux excitations can always move in any direction and the GSD only depends on the topology of the spatial manifold.

In contrast to liquid topological order, the X-cube model is very sensitive to lattice geometry. For example, on the cubic lattice there are three kinds of dimension-1 particles, which are constrained to only move along the x, y, and z-axis. However, when the X-cube model is defined on a stack of kagome lattices (Fig. 3b), there are *four* kinds of dimension-1 particles corresponding to the four different directions that the links of the lattice are aligned. These four kinds of dimension-1 particles are physically distinct; they belong to different superselection sectors and can be distinguished by braiding pairs of fractons from a distance (similar to how braiding can be done on a cubic lattice Fig. 1a).

As a more exotic lattice example, we can consider curved i-surfaces which can produce curved lattices. For example, a collection of curved surfaces can produce lattices with hyperbolic geometry (Fig. 5). On this lattice, the dimension-1 particles move along curved lines, which are geodesics of the hyperbolic plane. Thus, the mobility restrictions of the subdimensional particles inherit the geometry of the lattice. As a result, the rigid braiding operators (Fig. 1a-b) also inherit the lattice geometry.

The geometry-dependent mobility restrictions of the subdimensional particles also affects the ground state degeneracy (GSD). This is because, similar to toric code, the GSD of the X-cube model can be understood as resulting from non-local logical operators that act on the

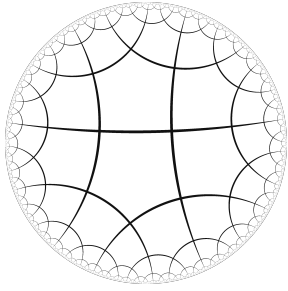


FIG. 5. Order-4 pentagonal tiling of the hyperbolic plane. A stack of this lattice can be created from the intersecting surface construction. The dimension-1 particles move along the lines of the above lattice, which are geodesics of the hyperbolic plane. As a result, the braiding operators in Fig. 1 will curve with the lattice geometry. The geometry of a hyperbolic 3-space can be constructed from an order-4 dodecahedral honeycomb [39].

degenerate ground state Hilbert space. These non-local operators are anticommuting Wilson and 't Hooft loops which correspond to moving a dimension-1 particle or a dimension-2 fracton pair, respectively, around a closed loop (Fig. 6a) [34, 40]. [[41]] Thus, the Wilson and 't Hooft loops share the geometric mobility constraints of the subdimensional particles. Since the 't Hooft loops are bound to a 2-dimensional i-surface, they are very similar to 't Hooft loops in 2d toric code. As a result, the GSD typically scales as

$$\log_2 \text{GSD} \sim \sum_s 2g_s \quad (3)$$

where \sum_s sums over all i-surfaces which each contribute a factor of 2^{2g_s} to the GSD, where g_s is the genus of the i-surface, s [[42]].

The geometry dependence of the Wilson and 't Hooft loops allows us to better understand a previous result that lattice curvature can lead to a robust GSD on a manifold with trivial topology [34]. The lattice considered is formed by constructing the cubic lattice from orthogonal i-surfaces (Fig. 3a) and then adding an additional large i-surface with the topology of a torus (Fig. 6b). The new torus-shaped i-surface has genus $g = 1$ and results in closed Wilson and 't Hooft loop operators around the torus, which contributes a factor of four to the GSD (in accordance with Eq. (3)). The GSD is robust in the limit of a large torus-shaped i-surface. Note that the topology of the spatial manifold wasn't changed; instead, it was argued in Ref. [34] that the resulting lattice should be interpreted as having spatial curvature around the torus-shaped i-surface.

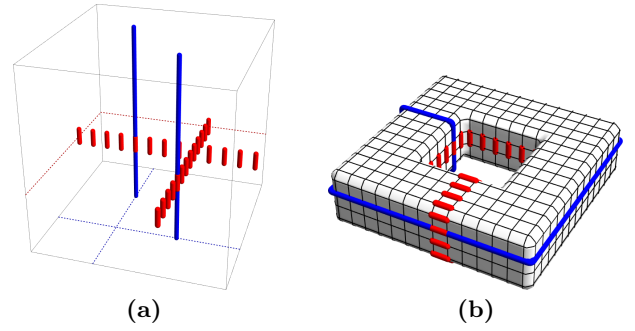


FIG. 6. (a) Wilson (blue) and 't Hooft loops (red) of the X-cube model on a cubic lattice, which are the logical operators that act on the degenerate ground state manifold [34, 40]. These loops are products of Z (blue) and X (red) operators. Physically, a Wilson loop moves a dimension-1 particle, while a 't Hooft loop moves a dimension-2 pair of fractons. (b) When a large torus-shaped i-surface is added to a cubic lattice (hidden for clarity), new links (black) with new qubits are added to the model. New Wilson and 't Hooft loops result on the torus-shape i-surface, which results in a GSD that can be attributed to lattice curvature. [34]

IV. MOBILIZING FRACTONS

We will now consider two lattices with a very large amount of positive curvature. The first lattice is a stack of the lattice shown in Fig. 7, which is constructed from cylinder-shaped i-surfaces. Note that on this lattice, we must also include the new loop terms in $H_{X\text{-cube}}$ (Eq. (2), Fig. 4b-c). These terms don't commute with Wilson and 't Hooft string operators (Fig. 6a) that are orthogonal to the plane, which prevents the subdimensional excitations from moving out of the plane. The lattice geometry does not support fractons, but instead results in a phase that is equivalent to a stack of 2+1d toric codes. String operators that move the toric code charges and fluxes are shown in Fig. 7.

Now consider a lattice constructed from spherical i-surfaces. We will place the spheres on a face-centered cubic (FCC) lattice (Fig. 8a-b). [[43]] Remarkably, when the X-cube model is defined on this lattice [[44]] the phase is equivalent to 3+1D Z_2 gauge theory (which can be described by BF theory or 3+1D toric code). [[45]] The important physics results from the fact that the lattice curvature allows the excitations of the 3-cell operators to be fully mobile, rather than immobile fractons which is the case on a cubic lattice. The excitations of the 3-cell operators are charge excitations (in the Z_2 gauge theory). A cross operator (Fig. 2b) excitation corresponds to a Z_2 gauge theory flux excitation, where a circle with an odd number of cross operator excitations on it been penetrated by a flux string. Logical operators are given in Ref. [23], which are useful for understanding the flux excitation.

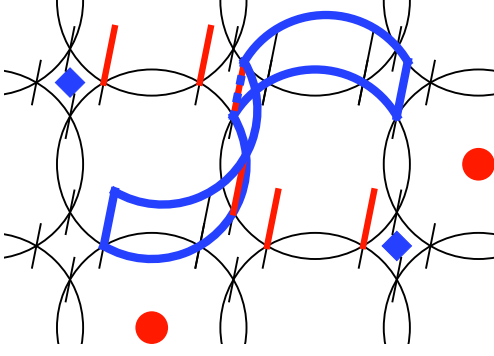


FIG. 7. The X-cube model on a stack of the above lattice results in a phase equivalent to a stack of 2+1D toric codes. Toric code charges (blue diamonds) and fluxes (red disks) are created at the ends of string operators which are products of X (red) and Z (blue) operators, respectively. A charge is an excitation of a cube-shaped 3-cell (e.g. at a blue diamond). A flux is an excitation of cross (Fig. 2b) and loop (Fig. 4c) operators. There are no fractons; the lattice curvature granted fractons mobility and turned them into toric code charges.

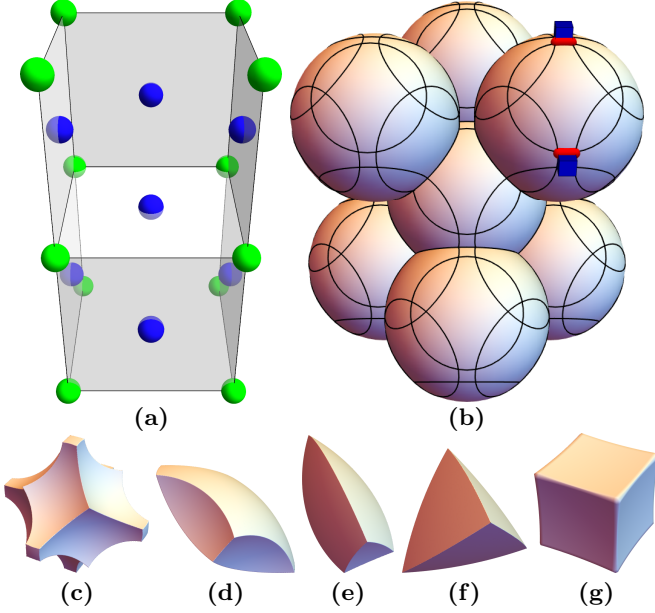


FIG. 8. (a) Part of a face-centered cubic (FCC) lattice (green and blue points). (b) Spherically-shaped i-surfaces (with radius 0.46) are placed at the vertices of the FCC lattice. Here, we show seven i-surfaces positioned at the seven blue points in (a). Qubits live on the lattice links (black) where two i-surfaces intersect. (Some links are hidden behind the spheres.) (c-g) The resulting 3-cells (3D volume enclosed by i-surfaces). The phase of the X-cube model on the resulting lattice is 3+1D Z_2 gauge theory. Excitations of the 3-cell cubes (g) are Z_2 charges (not fractons). The hopping operator is a product of X operators on the two red links in (b), which excites the two nearby blue cubes.

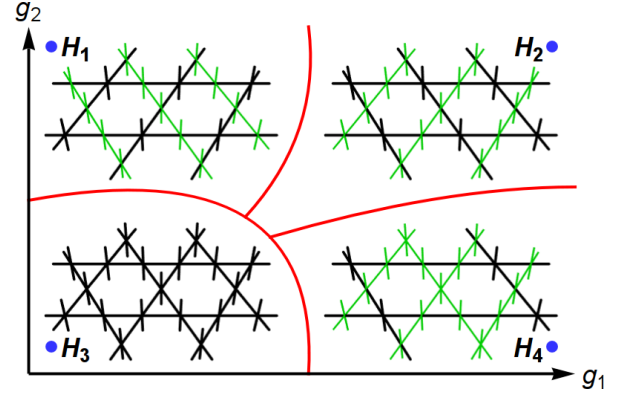


FIG. 9. A schematic phase diagram of $H(g_1, g_2)$ (Eq. (4)), which interpolates between the four Hamiltonians H_i ($i = 1, 2, 3, 4$) at the four corners (blue dots). Each H_i consists of the X-cube model defined on the black lattice (next to each H_i), while the qubits on the green links are trivially gapped out as in Eq. (4). The X-cube model is sensitive to the geometry of the lattice on which it is defined (black lattice), and as a result, each H_i belongs to a different phase and the four H_i are separated by phase transitions (red lines). This physics is unique to fracton order; if we placed a liquid topological order (e.g. 3d toric code) on the black lattice (instead of the X-cube model), then the above phase transitions would not be necessary.

V. DIFFERENT PHASES

We have shown that lattice geometry greatly affects the topological excitations, ground state degeneracy (GSD), and phase of the X-cube model. In this section we will discuss more subtle ways that the lattice geometry affects the phase of matter (Fig. 9).

We will use the physically motivated definition of phase of matter defined in Ref. [35]. Ground states of gapped local Hamiltonians are grouped into equivalence classes, which are interpreted as phases of matter. The ground states of $H(0)$ and $H(1)$ are in the same phase if there exists an adiabatic evolution of Hamiltonians $H(g)$ such that $H(g)$ is gapped for all $0 \leq g \leq 1$ (i.e. no phase transition occurs) where g parametrizes the coupling constants in $H(g)$. Equivalently, two states are in the same phase if they can be connected by a finite local unitary transformation. [[46]] [35]

We will argue that different lattice geometries result in different phases using two different kinds of arguments. The first argument is to consider the GSD. If two Hamiltonians have different GSD, then the Hamiltonians must be separated by a gap closing (i.e. a phase transition) so that the GSD can change. This implies that e.g. the X-cube model on the following lattices must correspond to different phases: a cubic lattice, a stacked kagome lattice, or a cubic lattice with a larger unit cell (Fig. 9).

To make this explicit, we can consider an arbitrary

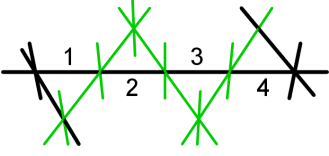


FIG. 10. Vertices of the black slanted cubic lattices in Fig. 9 can be separated by two or four black links. In order to define an X-cube model on these black lattices with extra degrees of freedom, we need to add an additional term to H_i (Eq. (4)), which takes the following form for the above for labeled links: $\sum_{\ell, \ell' \in \text{splitted black}} X_\ell X_{\ell'} = X_1 X_2 + X_1 X_3 + X_1 X_4 + X_2 X_3 + X_2 X_4 + X_3 X_4$.

interpolation $H(g_1, g_2)$ between four Hamiltonians H_i with $i = 1, 2, 3, 4$:

$$H_i = H_{\text{X-cube}}(\text{black}) - \sum_{\ell, \ell' \in \text{splitted black}} X_\ell X_{\ell'} - \sum_{\ell \in \text{green}} Z_\ell \quad (4)$$

$H(g_1, g_2)$ interpolates between H_i with $i = 1, 2, 3, 4$

Each H_i is defined on a stacked kagome lattice and consists of the X-cube model defined on the black lattice (next to each H_i in Fig. 9), while the qubits on the green links are trivially gapped out. The second term is not conceptually important and will be discussed in the next paragraph. For a periodic stacked kagome lattice of length L , H_1 and H_2 describe the X-cube model on different slanted cubic lattices and with a GSD $= 2^{6L-3}$. H_3 describes the X-cube model on a stacked kagome lattice with GSD $= 2^{8L-3}$. And H_4 describes the X-cube model on a slanted cubic lattice with a larger unit cell and GSD $= 2^{5L-3}$. [[47]] Thus, H_1 (and H_2), H_3 , and H_4 must belong to different phases since they have different GSD. [[48]]

There is a minor subtlety regarding the definition of $H_{\text{X-cube}}(\text{black})$ due to the fact that pairs of neighboring vertices in the black slanted cubic lattices (in Fig. 9) are split into multiple links (Fig. 10) on the stacked kagome lattice. In $H_{\text{X-cube}}(\text{black})$, the 3-cell operators are products of Z operators on all of the black links on the edge of a 3-cell. The cross operators are still products of exactly four X operators on four black links neighboring a vertex. The second term in Eq. (4) sums over all pairs of links that are between two neighboring vertices in a black lattice; see Fig. 10 for an example. We emphasize that H_1 is the same phase as the X-cube model defined on a slanted cubic lattice like the one that H_1 is defined on, but without the green links or multiple black links between neighboring vertices; H_1 just includes extra qubit degrees of freedom which are either gapped out (as in the green links) or sewed in using a local unitary (as in the splitted black links).

The two different slanted cubic lattices (H_1 and H_2) also belong to different phases. Again, this can

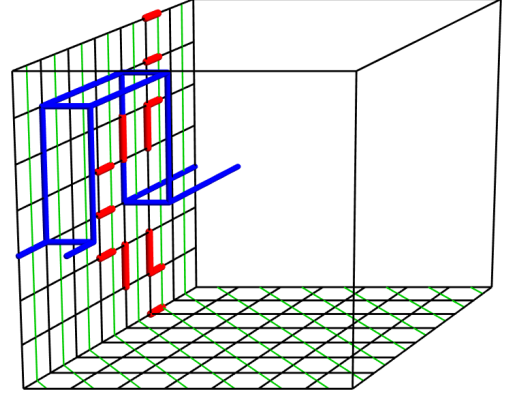


FIG. 11. A 't Hooft loop (red) and paired Wilson loop (blue), which both commute with H_1 (Fig. 9) (but not H_2). The 't Hooft and paired Wilson loop operators anticommute and are products of X and Z operators on the red and blue links, respectively. The above loop operators each transport dimension-2 particles around a periodic direction via a non-linear path. H_2 does not have topological excitations that can traverse the same plane (which becomes a precise statement in the limit of large system size). In Appendix A 2, we use this fact to argue that H_1 and H_2 correspond to different phases of matter.

be shown using certain choices of periodic boundary conditions for which these Hamiltonians have different GSD (Appendix A 1). However, there is also a physical reason for different phases. The dimension-2 particles (i.e. pairs of fractons or dimension-1 particles) are bound to a i-surface (plane of the black cubic lattice in this case), and these i-surfaces are different in H_1 and H_2 . If we consider a 't Hooft loop or paired Wilson loop formed by these dimension-2 particles, then there are loop operators (Fig. 11) that only exist in H_1 or H_2 , but not both. In Appendix A 2, we use this intuition to show more formally that in general it is not possible to relate the ground states of H_1 and H_2 by a local unitary transformation. H_1 and H_2 can be related by a lattice rotation, but this is not a local unitary transformation. Thus, the X-cube model on a rotated lattice can result in a different phase of matter from the X-cube model on the un-rotated lattice. [[49]]

VI. CONCLUSION

We have shown that nearly all important characterizations of the long distance physics of the X-cube model depend on lattice geometry. These characterizations include: the mobility restrictions of the topological excitations and braiding operators, ground state degeneracy, and the phase of matter. We emphasize that liquid topological order is blind to lattice geometry in the sense that none of the above characteristics of liquid topological order depends on the geometry of the lattice. Thus, we

propose that fracton orders should be regarded as a *geometric order* to emphasize the important role played by geometry.

However, we have only briefly studied examples of how geometry affects the physics of the X-cube model. A more complete and general understanding of the generic mathematical structure would be very desirable. For example, if the X-cube model is the simplest example of fracton order in the same way that toric code is the simplest example of topological order, more interesting geometric physics may emerge in other fracton models, similar to how more interesting topological invariants result from more exotic models of (liquid) topological order [8].

Previously proposed emergent gravity models [50–54] where later discovered to actually be gapless fracton models [33]. And recently, a gravity-like attraction mechanism between fractons was discovered [33] in gapless $U(1)$ fracton models [21, 55] (although the attractive force is only long ranged if the model has gapless fracton dipoles). These gapless $U(1)$ fracton models therefore appear to be simplified versions of a gravity-like model. The gapped Z_N fracton models discussed in this work are the discrete analogs of the $U(1)$ fracton models. It would therefore be interesting to study how the geometry-dependent physics discussed in this work applies to the $U(1)$ fracton models, and how the gravity-like connections of the $U(1)$ fracton models may apply to the gapped Z_N fracton models.

We thank Wilbur Shirley, Xie Chen, Zhenghan Wang, Michael Pretko, Tim Hsieh, Wonjune Choi, and Dave Aasen for helpful and encouraging discussions. This work was supported by the NSERC of Canada and the Center for Quantum Materials at the University of Toronto.

[1] Topological excitations can not be annihilated by local operators, but instead require contact with a corresponding antiparticle in order to be annihilated. Examples include ordinary electrons and the charge and flux excitations of toric code [6].

[2] B. Zeng and X.-G. Wen, *Phys. Rev. B* **91**, 125121 (2015).

[3] A. Kitaev, *Annals of Physics* **321**, 2 (2006), January Special Issue.

[4] X.-G. Wen, *National Science Review* **3**, 68 (2016).

[5] T. Lan, L. Kong, and X.-G. Wen, *arXiv:1704.04221* (2017).

[6] A. Kitaev, *Annals of Physics* **303**, 2 (2003).

[7] M. Blau and G. Thompson, *Annals of Physics* **205**, 130 (1991).

[8] P. Putrov, J. Wang, and S.-T. Yau, *Annals of Physics* **384**, 254 (2017).

[9] S. Vijay, J. Haah, and L. Fu, *Phys. Rev. B* **92**, 235136 (2015).

[10] J. Haah, *Phys. Rev. A* **83**, 042330 (2011).

[11] B. Yoshida, *Phys. Rev. B* **88**, 125122 (2013).

[12] C. Chamon, *Phys. Rev. Lett.* **94**, 040402 (2005).

[13] S. Bravyi, B. Leemhuis, and B. M. Terhal, *Annals of Physics* **326**, 839 (2011).

[14] S. Vijay, J. Haah, and L. Fu, *Phys. Rev. B* **94**, 235157 (2016).

[15] S. Vijay and L. Fu, *arXiv:1706.07070* (2017).

[16] H. Ma, E. Lake, X. Chen, and M. Hermele, *Phys. Rev. B* **95**, 245126 (2017).

[17] T. H. Hsieh and G. B. Halász, *Phys. Rev. B* **96**, 165105 (2017).

[18] G. B. Halász, T. H. Hsieh, and L. Balents, *arXiv:1707.02308* (2017).

[19] O. Petrova and N. Regnault, *arXiv:1709.10094* (2017).

[20] B. J. Brown, D. Loss, J. K. Pachos, C. N. Self, and J. R. Wootton, *Rev. Mod. Phys.* **88**, 045005 (2016).

[21] M. Pretko, *Phys. Rev. B* **95**, 115139 (2017).

[22] T. Devakul, S. A. Parameswaran, and S. L. Sondhi, *arXiv:1709.10071* (2017).

[23] W. Shirley, K. Slagle, Z. Wang, and X. Chen, (2017).

[24] B. Shi and Y.-M. Lu, *arXiv:1705.09300* (2017).

[25] H. Ma, A. T. Schmitz, S. A. Parameswaran, M. Hermele, and R. M. Nandkishore, *arXiv:1710.01744* (2017).

[26] A. T. Schmitz, H. Ma, R. M. Nandkishore, and S. A. Parameswaran, *arXiv:1712.02375* (2017).

[27] A. Prem, J. Haah, and R. Nandkishore, *Phys. Rev. B* **95**, 155133 (2017).

[28] M. Pretko, *Phys. Rev. B* **96**, 115102 (2017).

[29] M. Pretko and L. Radzihovsky, *arXiv:1711.11044* (2017).

[30] D. J. Williamson, *Phys. Rev. B* **94**, 155128 (2016).

[31] K. Slagle and Y. B. Kim, *arXiv:1704.03870*.

[32] J. Haah, *Phys. Rev. B* **89**, 075119 (2014).

[33] M. Pretko, *Phys. Rev. D* **96**, 024051 (2017).

[34] K. Slagle and Y. B. Kim, *Phys. Rev. B* **96**, 195139 (2017).

[35] X. Chen, Z.-C. Gu, and X.-G. Wen, *Phys. Rev. B* **82**, 155138 (2010).

[36] M. B. Hastings, *arXiv:1008.5137* (2008).

[37] (), in [14], a Z_N generalization of the X-cube model was given. However, their Z_N model only generalizes to lattices with bipartite 3-cells. That is, the vertices of every 3-cell must form a bipartite lattice. In our figures, we present an alternative Z_N generalization which does not require bipartite 3-cells. However, our generalization has a peculiarity where odd integer system sizes can result in a reduced GSD. For simplicity, we will focus on the Z_2 model in the main text, for which $X^\dagger = X$.

[38] It is possible to have 3-cells and loops that get arbitrarily large. In order to keep the Hamiltonian local, the coefficients of the 3-cell and loop operators in Eq. (2) should decay exponentially with the size of the operator.

[39] wikipedia.org/wiki/Order-4_dodecahedral_honeycomb.

[40] H. He, Y. Zheng, B. A. Bernevig, and N. Regnault, *arXiv:1710.04220* (2017).

[41] The non-local logical operators for toric code are also Wilson and 't Hooft loops which correspond to moving charges and fluxes, respectively, around non-contractible closed loops.

[42] If the i-surface s in Eq. (3) is not connected and orientable, then $2g_s$ should be replaced by the first Betti number with Z_2 coefficients.

[43] Placing the spheres on a cubic lattice results in four spheres intersecting at a single point, which violates the assumptions of our lattice construction.

[44] In this case the new loop terms in $H_{X\text{-cube}}$ (Eq. (2), Fig. 4b-c) are actually optional.

[45] Indeed, we have checked that the degeneracy is 8 for the

X-cube model on the intersecting spheres lattice (Fig. 8) with periodic boundary conditions. [[47]] The unit cell is composed of 48 links on which the Pauli operators reside.

- [46] Finite local unitary transformations can be generated by a finite time evolution of a local time-dependent Hamiltonian. Note that it is allowed (and sometimes necessary) to add extra degrees of freedom to $H(g)$ (and thus also to $H(0)$ and $H(1)$) as long as these extra degrees of freedom are gapped and decoupled when $g = 0$ or $g = 1$.
- [47] (), ground state degeneracies were calculated using a method equivalent to the method described in Appendix B of Ref. [16].
- [48] However, in Ref. [23] it is shown that a local unitary transformation can connect H_2 to the union of H_4 and decoupled stacks of toric code.
- [49] A translated a lattice, by e.g. half of a unit cell, does not result in a different phase since a lattice translation is a local unitary transformation.
- [50] Z.-C. Gu and X.-G. Wen, [arXiv:gr-qc/0606100](#) (2006).
- [51] Z.-C. Gu and X.-G. Wen, *Nuclear Physics B* **863**, 90 (2012).
- [52] C. Xu, [arXiv:cond-mat/0602443](#) (2006).
- [53] C. Xu, *Phys. Rev. B* **74**, 224433 (2006).
- [54] C. Xu and P. Hořava, *Phys. Rev. D* **81**, 104033 (2010).
- [55] A. Rasmussen, Y.-Z. You, and C. Xu, [arXiv:1601.08235](#) (2016).
- [56] Recall that if it were possible to distinguish $|\psi_1\rangle$ and $|W_1\psi_1\rangle$ using the expectation value of a local operator H' , then H' could be added to the Hamiltonian H_1 with an arbitrarily small coefficient and split the degeneracy between $|\psi_1\rangle$ and $|W_1\psi_1\rangle$, which is impossible because the ground state degeneracy of the X-cube model on a periodic cubic lattice is robust to perturbations [14].

Appendix A: Rotated Lattice Arguments

In this appendix, we will argue more thoroughly that the X-cube model on lattices that only differ by a rotation can result in different phases of matter. As a concrete example, we will show that the ground states of H_1 and H_2 (Fig. 9) belong to different phases. We now want to show that these two gapped Hamiltonians correspond to different phases of matter; i.e. the Hamiltonians must be separated by a phase transition and their ground states can not be related by a finite local unitary transformation.

1. Degeneracy Argument

First, we will give an example of a certain periodic boundary condition for which the two Hamiltonians (H_1 and H_2) have a different ground state degeneracies (GSD). A periodic lattice can be defined by imposing a periodic equivalence of lattice points. A typical choice for a lattice of lengths (L_1, L_2, L_3) is to equate each point \mathbf{x} as follows:

$$\mathbf{x} \equiv \mathbf{x} + L_1 \mathbf{a} \equiv \mathbf{x} + L_2 \mathbf{b} \equiv \mathbf{x} + L_3 \mathbf{c} \quad (\text{A1})$$

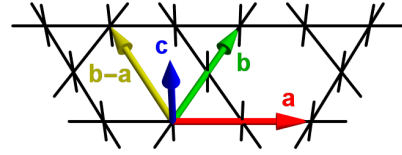


FIG. 12. Lattice vectors used to define the periodic boundary conditions in Eq. (A1) and (A2).

where \mathbf{a} , \mathbf{b} , and \mathbf{c} are lattice vectors. With the lattice vectors shown in Fig. 12, the above periodic boundary conditions result in a $\log_2 \text{GSD} = 2L_1 + 2L_2 + 2L_3 - 3$ for both H_1 and H_2 .

However, if we instead choose

$$\mathbf{x} \equiv \mathbf{x} + \mathbf{b} + L_1 \mathbf{a} \equiv \mathbf{x} + L_2 \mathbf{b} \equiv \mathbf{x} + L_3 \mathbf{c} \quad (\text{A2})$$

then H_1 has $\log_2 \text{GSD} = 2L_2 + 2L_3$ (for even L_1) while H_2 instead has a much smaller $\log_2 \text{GSD} = 2 + 2L_3$ (for even L_1 and L_2) [[47]]. The reduced GSD occurs because the Wilson loops along certain directions (Fig. 6a) get merged into a single Wilson loop due to the shifted periodic boundary condition. Since H_1 and H_2 have different GSD on the same lattice, they must be separated by a phase transition.

2. Logical Operator Argument

As an alternative argument, we will derive a contradiction by assuming that the ground states of H_1 and H_2 (Eq. (4)) can be related by a local unitary transformation (in the sense of Ref. [35]). We will work in the limit of an infinitely large lattice so that the concept of local operators is well-defined. This will not be a proof since we will apply the physics knowledge that H_2 does not have mutual semion topological excitations that can traverse the loops in Fig. 11.

To derive a contradiction, consider a ground state $|\psi_1\rangle$ of H_1 that is an eigenstate of the 't Hooft loop T_1 in Fig. 11, which wraps a dimension-2 particle (composed of a pair of fractons) around a periodic direction. We will also consider the paired Wilson loop operator W_1 in Fig. 11, which wraps a dimension-2 particle (composed of a pair of dimension-1 particles) around the same plane. The algebra of these operators is

$$T_1 |\psi_1\rangle = |\psi_1\rangle \quad T_1 W_1 = -W_1 T_1 \quad (\text{A3})$$

To derive a contradiction, suppose that H_2 has a ground state $|\psi_2\rangle$ that is related to $|\psi_1\rangle$ by a finite local unitary transformation U via $|\psi_2\rangle = U|\psi_1\rangle$. We can then define the transformed operators

$$T_2 \equiv U T_1 U^{-1} \quad W_2 \equiv U W_1 U^{-1} \quad (\text{A4})$$

$|W_2\psi_2\rangle \equiv W_2|\psi_2\rangle$ must also be a ground state of H_2 . This is because

$$\begin{aligned} \langle\psi_2|H_2^n|\psi_2\rangle &= \langle\psi_1|U^{-1}H_2^nU|\psi_1\rangle \\ &\parallel \\ \langle W_2\psi_2|H_2^n|W_2\psi_2\rangle &= \langle W_1\psi_1|U^{-1}H_2^nU|W_1\psi_1\rangle \end{aligned} \quad (\text{A5})$$

where we have raised H_2 to a positive integer power n . The right hand sides of the above two lines must be equal since $|\psi_1\rangle$ and $|W_1\psi_1\rangle \equiv W_1|\psi_1\rangle$ are ground states of H_1 (which is topologically ordered) and must therefore be indistinguishable by local operators [[56]], and $U^{-1}H_2^nU$ is a local operator (since H_2 and U are local). Using $n = 1$ and $n = 2$, Eq. (A5) shows that $|\psi_2\rangle$ and $|W_2\psi_2\rangle$ have the same energy expectation value and energy uncertainty of H_2 . Since $|\psi_2\rangle$ is a ground state of H_2 with zero energy uncertainty, $|W_2\psi_2\rangle$ is therefore also a ground state of H_2 .

Therefore, T_2 and W_2 are logical operators that act on the ground states $|\psi_2\rangle$ and $|W_2\psi_2\rangle$ of H_2 with the

following algebra

$$T_2|\psi_2\rangle = |\psi_2\rangle \quad T_2W_2 = -W_2T_2 \quad (\text{A6})$$

since $|\psi_2\rangle = U|\psi_1\rangle$. But since U is local, T_2 and W_2 must only act on the qubits near the (red and blue) loops drawn in Fig. 11. However, H_2 does not have logical operators obeying Eq. (A6) that only act in this region. This is because the presence of these string logical operators would imply the existence of topological excitations that can move along the loops drawn in Fig. 11. However, no such excitations exist for H_2 . We have thus derived a contradiction by assuming that the ground states of H_1 and H_2 can be related by a finite local unitary transformation. Therefore, the ground states of H_1 and H_2 can't be related by a finite local unitary transformation and must therefore correspond to different phases of matter.

Note that in order to derive a contradiction it was essential that we assumed that U is a *local* transformation. In particular, U can not be a $2\pi/3$ lattice rotation operator and thus T_2 and W_2 can not simply be equal to T_1 and W_1 rotated by $2\pi/3$.